*International Journal of Innovative Computing, Information and Control*
Volume **9**, Number **6**, June **2013**

ICIC International ©2013 ISSN 1349-4198
pp. 2585–2596

# ADVANCED CONTROL OF ON-SHIP SOLAR TRACKER USING ADAPTIVE WIDE RANGE ANFIS

Budhy Setiawan[1,2], Mauridhi Hery Purnomo[1], Mochamad Ashari[1] and Takashi Hiyama[3]

[1]Department of Electrical Engineering
Sepuluh Nopember Institute of Technology (ITS)
Surabaya 60111, Indonesia
stbuddy@yahoo.com

[2]Department of Electrical Engineering
Politeknik Negeri Malang
Malang 65144, Indonesia

[3]Department of Computer Sciences and Electrical Engineering
Kumamoto University
Kumamoto 860-8555, Japan

Received March 2012; revised July 2012

Abstract. *Problem of a tracker on a ship is to maintain focus accuracy to point the sun on nonlinear and time variant disturbance condition, which is caused by ship's rotational movements. The tracker requires a suitable x-y axes Cartesian mechanical system and an adaptive control method. In this paper, we propose an Adaptive Wide Range ANFIS (Adaptive Neuro Fuzzy Inference System) method to compensate the sun angle trajectory toward vessel movements of an on-ship solar tracker. Meanwhile, in the previous research, conventional method performed instability in handling time variant disturbance. This paper develops model of an on-ship tracker, vessel's rotational movements and ANFIS control. ANFIS input consists of two group, which are target position and base disturbance position. ANFIS is trained using conventional method, but under various condition and adjustment. As a result, the proposed control performs significant stability, engine vibration immunity, and wide range time variant response in achieving focus accuracy on a traveling ship simulation with 0.0028 percent error.*
**Keywords:** On ship solar tracker, x-y Cartesian, Adaptive wide range ANFIS

1. **Introduction.** On-ship solar tracker is parameterized mainly by nonlinear and time variant disturbances. The parameters are caused by the ship's rotational movements. In application, the Cartesian tracker is mounted by a High Concentrated Photovoltaic (HCPV) panel [1]. The HCPV has conversion efficiency up to 41 percent. Consequently, the HCPV panel requires a solar tracker with an adaptive control, so that the HCPV can always point the sun to get maximum energy. Otherwise, the energy may reduce significantly [2, 3].

Previous researches on solar tracker used two axes Cartesian solar tracker stand on fixed base applications (on the ground). Most of them apply on/off method [4, 5]. Their maximum focus error is 0.05° [4, 5, 6, 7, 8, 9]. The latest improved method on the fixed base has been done by Louchene in 2007 using artificial intelligent, Fuzzy single tone. In his research, the method shows its stability and smoothness in tracking the sun [10]. However, the method has never been used on mobile tracker.

In 2009, an analytical and simulation approach for mobile base solar tracker had been investigated for its focus maximization using geometric 3D vector objects method. The

tracker is controlled by on/off control method and based on application of 6 light sensors [11]. In the same year, an analytical investigation on involved parameter of the sun tracking from a ship results on two axes Cartesian solar tracker formulas. The Cartesian axes are affected directly by sun tracking inputs and disturbed by ship rotational motions, such as pitch, roll and yaw [1].

Following the research, an investigation on conventional control for on-ship solar tracker shows a simplicity in design and fast response, but also incapability in compensating any ship engine vibration and high slope degree inputs [12].

Because of the complexity of this tracker system, an adaptive compensation method may be used for achieving a better performance. There are some adaptive methods which can be applied, such as Adaptive PID, Adaptive Fuzzy [13], and ANFIS [14].

This paper proposes an Adaptive Wide Range ANFIS to control the on-ship solar tracker. The simulation is conducted to rough wave disturbance, engine vibration and step angle input.

2. **Proposed Method.** On ship solar tracker is a mechanism that consists of a HCPV panel, as shown on Figure 1. The panel is mounted on an X-Y Cartesian solar tracker, and the tracker is attached on a ship. In order to reach the sun position, an X axis rotational movement of the solar tracker has to be in line to the ship's longituginal x axis. And a Y axis is parallel to ship's transfersal y axis. The sun is a moving target, and the ship is a moving base [1].

The proposed control system for the tracker consists of two blocks, the calculation block and ANFIS controller block, as shown on Figure 2. Inputs of the calculation block are sun pointer pairs ($L_y$ - $L_{-y}$ and $L_x$ - $L_{-x}$), as mobile target inputs. And, mobile base inputs are ship movements, comprising roll ($\phi$), pitch ($\theta$) and yaw ($\psi$). Beside the movement, there are some engine vibrations, which are known as $\varpi_y$ and $\varpi_x$ are also the inputs. In application, all of those input variables are taken from some sensors. However, in simulation, models of the inputs are developed.

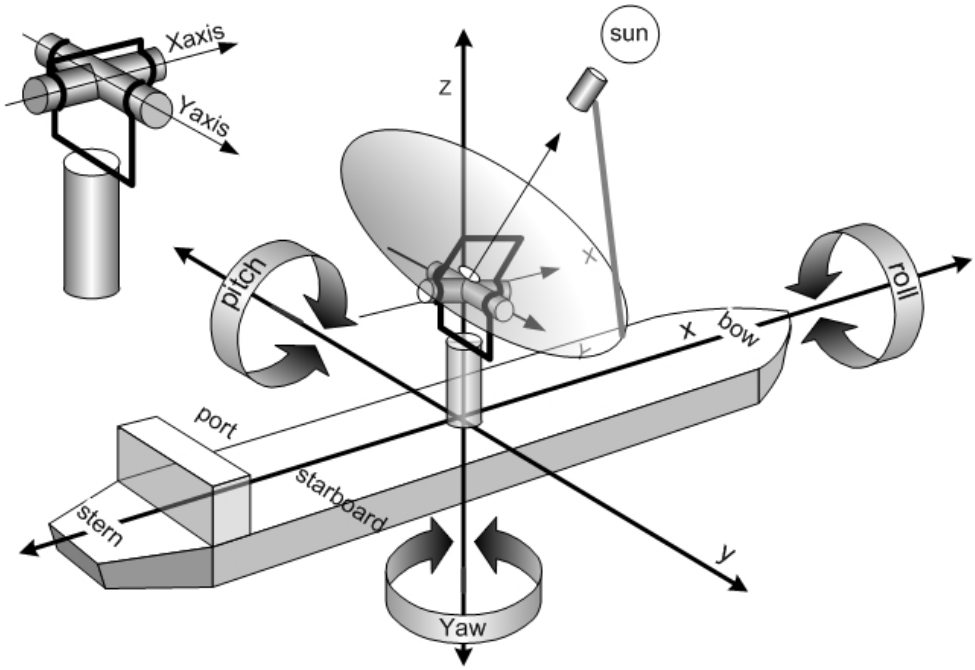


FIGURE 1. On-ship cartesian solar tracker system [1,14]

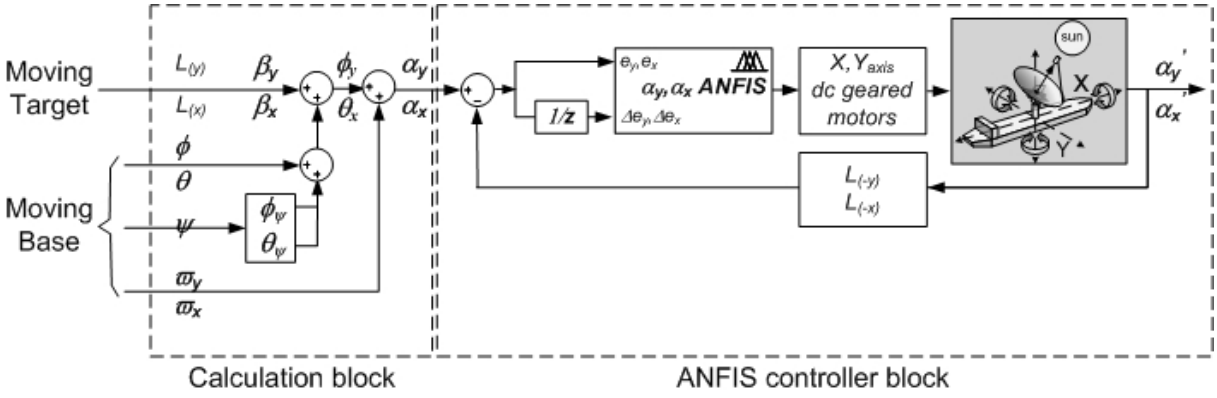


FIGURE 2. Adaptive wide range ANFIS

The other block is ANFIS controller. It has two inputs, $\alpha_y$ and $\alpha_x$ which are fed by the previous block. The outputs of ANFIS controllers consist of $\alpha_y^{'}$ and $\alpha_x^{'}$. An ANFIS controls X axis angle of the sun tracker, $(\alpha_y^{'})$. And, the other one compensates Y axis angle $(\alpha_x^{'})$. Each angle is represented by a geared dc motor.

3. **Modeling of the System.** The moving target and the moving base are calculated based on the following model.

3.1. **Moving target.** The moving target is the sun angles from a traveling ship. There are two major sun paths. The first path is the elevation trajectory, which moves from east to west in a day with 15°/hour angular speed. The second path is the altitude path that travels from 23.45° (north) to −23.45° (south) and back in a period of a year. In calculation, the elevation degree, $h_s$, is expressed as,

$$h_s = 15^{\circ} h_{sn} \tag{1}$$

where $h_{sn}$ = sidereal hour of a local site. A sidereal hour is a time scale that is based on the earth's rate of rotation measured relatively to the sun.

The altitude angle, $\delta_s$, is expressed as:

$$\delta_s = \left[23.45^{\circ} \sin\left(\left[360\frac{284+n}{365}\right]^{\circ}\right)\right] \tag{2}$$

where $n$ = a day number within a year, starting on the January 1st.

To get the sun's altitude angle $(\alpha)$ from a ship coordinate, an equation can be expressed as:

$$\sin(\alpha) = [\sin(L)\sin(\delta_s)\cos(L)\cos(\delta_s)\cos(h_s)] \tag{3}$$

and azimuth angle, $\alpha_s$, from equation:

$$\sin(\alpha_s) = \cos(\delta_s)\frac{\sin(h_s)}{\cos(\alpha)} \tag{4}$$

Finally, the ship at a certain latitude $(L)$, on day $(n)$ and sidereal time $(h_{sn})$ will give a form of angles altitude $(\alpha)$ and azimuth $(\alpha_s)$ [7]. Those given angles will directly affect the two pair of sun light sensors of the tracker to form sun angles, $\beta_y$ and $\beta_x$.

3.2. **Moving base.** Moving base is a traveling ship with its Rotational Movements. While facing the sun, the tracker has to deal with the ship's rotational movements, 3 degree of freedom (3 DoF). The 3 DoF is the main parameters to be significantly considered in mobile base control, as shown in Figure 1. Those three rotational movements are roll, pitch and yaw. Due to performing the proposed simulation, the movement models are developed.

Roll angle is a rotational movement on a ship's longitudinal x axis on z-y side. The roll movement is affected by ship kinematics such as roll damping, roll natural frequency, initial meta centric height, variation in wave, bias angle and keel [15].

Pitch angle is a rotational movement along the transversal y axes of a ship on z-x side. The pitch movement is affected by some ship kinematics parameters, such as elevation wave, artificial frequency and sea wave angle [16].

Yaw angle is a rotational movement of a ship on x-y side toward z axis. Yaw angle has smaller degree changing compare to roll and pitch, and has main significant variables as rudder angle, linear resultant of hydrodynamics derivation, virtual moment of ship's inertia and mass, and ship stability (stability index).

All of the ship's 3 DoF parameters are non linear, oscillated, time variant, uncertain, abrupt change and unpredictable [15, 16, 17, 18].

The sun pointing and ship's movement are more significant variables to be considered, rather than the sun trajectory and the ship traveling path,

3.3. **Axes properties.** In this research, a Cartesian solar tracker is constructed by two axes, known as X and Y, as shown in Figure 3. And, its variables are displayed on Table 1. The X axis' actuator angle ($\alpha_y$) works on two dimensional area, y-z side. The X axis is composed mainly by the y sun position ($\beta_y$) and roll degree ($\phi$). While the Y axis' actuator angle ($\alpha_x$) rotates on x-z plane. The Y axis is composed primarily by the x sun position ($\beta_x$) and pitch degree ($\theta$). Each axis equation is presented as follows:

$$X_{axis} \Rightarrow \alpha_y = \beta_y + \phi_y, \quad \{-90^\circ < \alpha_y < 90^\circ\} \tag{5}$$

$$Y_{axis} \Rightarrow \alpha_x = \beta_x + \theta_x, \quad \{-90^\circ < \alpha_x < 90^\circ\} \tag{6}$$

TABLE 1. Tracker control variables

| Var | X axis variables (y-z side) | Var | Y axis variables (x-z side) |
|---|---|---|---|
| $L_y$ | Starboard sun light (opto sensor) | $L_x$ | Bow sunlight (opto sensor) |
| $L_{-y}$ | Port sun light (opto sensor) | $L_{-x}$ | Stern (opto sensor) |
| $\beta_y$ | Sun to z input on y-z plane | $\beta_x$ | Sun to z on x-z plane of a ship |
| $\beta_y'$ | Sun to z response on y-z plane | $\beta_x'$ | Sun to z response on x-z plane |
| $\phi$ | Roll angle (deck gyrometer) | $\theta$ | Pitcfh angle (deck gyrometer) |
| $\phi_\psi$ | Roll angle by $\psi$ | $\theta_\psi$ | Pitch angle by $\psi$ |
| $\phi_y$ | Total roll angle ($\phi + \phi_\psi$) | $\theta_x$ | Total pitch angle ($\theta + \theta_\psi$) |
| $\alpha_y$ | y-z control input | $\alpha_x$ | x-z control input |
| $\varpi_y$ | y vibration angle (accelerometer) | $\varpi_x$ | x vibration angle (accelerometer) |
| $\psi$ | Yaw angle (deck gyrometer) | $\psi$ | Yaw angle (deck gyrometer) |
| $e_y$ | $\alpha_y$ ANFIS input error | $e_x$ | $\alpha_x$ ANFIS input error |
| $\Delta e_y$ | $\Delta\alpha_y$ ANFIS input error | $\Delta e_x$ | $\Delta\alpha_x$ ANFIS input error |
| $\alpha_y'$ | y-z angle output | $\alpha_x'$ | x-z angle output |

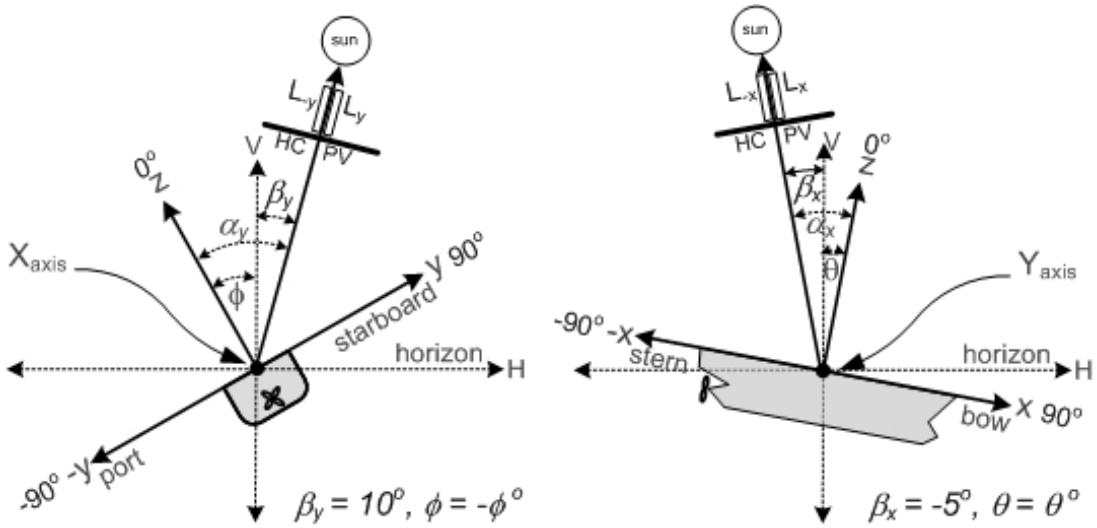


FIGURE 3. X and Y axes properties

Meanwhile the sun angles ($\beta_y$ and $\beta_x$) are accumulation degrees which are formed by every pair of sun light sensors in reaching equal value of sun intensity.

$$\beta_y^{'} \Leftarrow L_y - L_{-y}, \quad \left\{-90° < \beta_y^{'} < 90°\right\} \tag{7}$$

$$\beta_x^{'} \Leftarrow L_x - L_{-x}, \quad \left\{-90° < \beta_x^{'} < 90°\right\} \tag{8}$$

In addition, both axes' inputs are affected by ship's yaw rotational movement caused by maneuver or wave. In adapting the yaw angle, X and Y axes have to consider the converted yaw to y and x effected angles. In other words, yaw produces an affected roll angle ($\phi_\psi$) from its original roll ($\phi$) and an affected pitch ($\theta_\psi$) from its original ($\theta$).

$$\phi_\psi = \phi\left(\sin\left(\psi\right)\right) \tag{9}$$

$$\theta_\psi = \theta\left(1 - \cos\left(\psi\right)\right) \tag{10}$$

Both axes are also exaggerated by ship's engine vibrations. The ship engine vibrations are $\varpi_y$ align with X axis, and $\varpi_x$ align with Y axis in frequency range 0.5 – 100 Hz. Their relations to roll and pitch are:

$$\phi_y = \phi_\psi + \phi \tag{11}$$

$$\theta_x = \theta_\psi + \theta \tag{12}$$

So that, the input parameter of the $\alpha_y$ and $\alpha_x$ are

$$\alpha_y = \beta_y + \phi_y + \varpi_y \tag{13}$$

$$\alpha_x = \beta_x + \theta_x + \varpi_x \tag{14}$$

Finally, focus accuracy in facing the sun for X axis can be calculated as follows:

$$\beta_y = \alpha_y - \phi \tag{15}$$

$$\beta_y^{'} = \alpha_y^{'} - \phi \tag{16}$$

So that, the focus accuracy response for X axis can be formulated as:

$$Xfocus = \beta_y^{'} - \beta_y \tag{17}$$

And, the focus accuracy for Y axis can be formulated such as:

$$\beta_x = \alpha_x - \theta \tag{18}$$

$$\beta_x^{'} = \alpha_x^{'} - \theta \tag{19}$$

So that, the focus accuracy response for Y can be formulated such as:

$$Yfocus = \beta_x^{'} - \beta_x \tag{20}$$

Axes angle actuators used in the research are geared dc motors. As plants load for the control, the motors are capable to handle their current effective applied, reverse rotation and electrical breaking.

Math model of a geared dc motor is constructed of electrical circuit and mechanical equation. The electrical loop applies Kirchoff voltage and current and mechanical motor equations are formulated into a transfer function model as follows [19]:

$$\frac{\theta(s)}{V_s(s)} = \frac{67838427}{s(s+1.775x10^4)(s+2.65)} \tag{21}$$

4. **Control Design.** As shown on Figure 2, the proposed method consists of two identical ANFIS controllers. They are $\alpha_y$ ANFIS and $\alpha_x$ ANFIS controlllers. The ANFIS's method in the control are tracking error for the angle inputs $\alpha_y$, and $\alpha_x$.

The ANFIS configuration respects to the first order of Sugeno Fuzzy input model, $e_y$ and $\Delta e_y$. So that, as shown on Figure 4, the $\alpha_y$ ANFIS' inputs are $e_y$ and $\Delta e_y$, in which:

$$e_y = \alpha_y^{'} - \alpha_y \tag{22}$$

$$\Delta e_y = e_{y(t)} - e_{y(t-1)} \tag{23}$$

and the $\alpha_x$ ANFIS' inputs are $e_x$ and $\Delta e_x$, where:

$$e_x = \alpha_x^{'} - \alpha_x \tag{24}$$

$$\Delta e_x = e_{x(t)} - e_{x(t-1)} \tag{25}$$

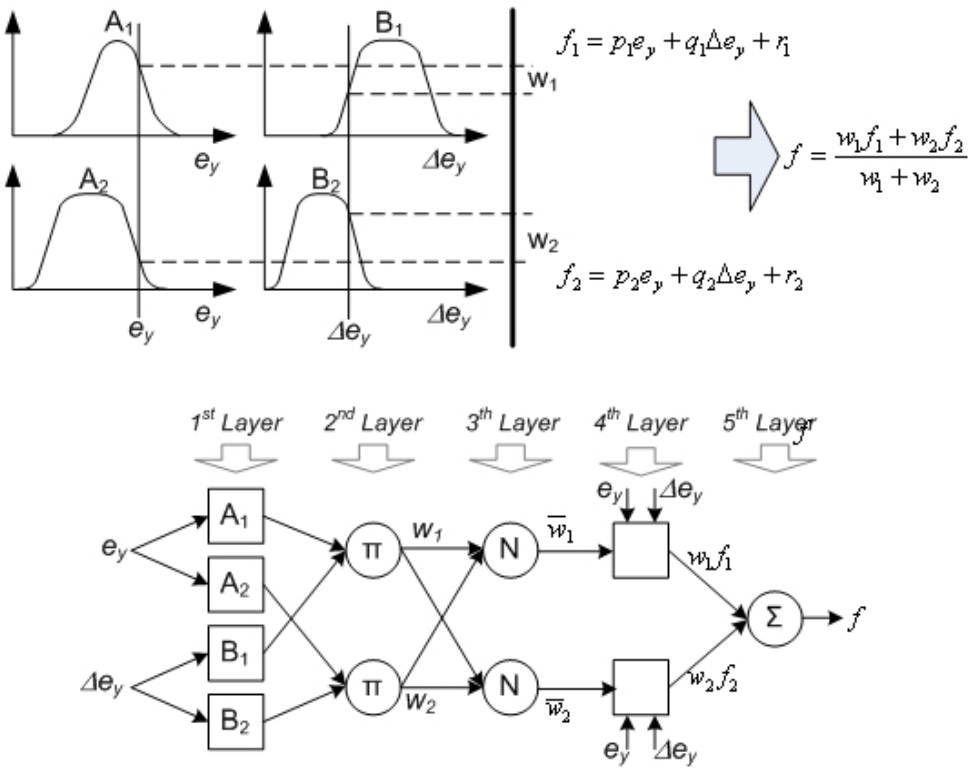


FIGURE 4. Adaptive Neuro fuzzy inference system

The basic rule set of the 'if then' fuzzy are as follows:

$$1^{\text{st}} \text{ Rule: If } e_y \text{ is } A_1 \text{ and } \Delta e_y \text{ is } B_1, \text{ then } f_1 = p_1 e + q_1 \Delta e_y + r_1 \tag{26}$$

$$2^{\text{nd}} \text{ Rule: If } e_y \text{ is } A_2 \text{ and } \Delta e_y \text{ is } B_2, \text{ then } f_2 = p_2 u + q_2 \Delta e_y + r_2 \tag{27}$$

Figure 4 shows defuzzification of Sugeno Fuzzy model and its neural network programming architecture. The program architecture of Sugeno has 5 layer processing, they are:

$1^{\text{st}}$ Layer, Defuzzification Layer. In the layer, every node is adaptive. The $e$ and $\Delta e$ are inputs for node $i$ and $A_i$ or $B_{i-2}$. The inputs are linguistic label that have some association with those nodes. The fuzzification membership function in this research applies Gaussian combination function.

$2^{\text{nd}}$ Layer, Product Layer. In the phase, product process of defuzzification happens. Different from the first layer, the $2^{\text{nd}}$ layer has some permanent nodes that represent a constant level for each rule. The layer output is product of all input signals. Each output node represents product of every rule. The layer uses AND association.

$3^{\text{rd}}$ Layer, Normalize Layer. Every node in this layer is permanent node with label N. Node $i$ counts result product ratio of the rule $i$ toward number of all output result. The layer is known as Normalized firing strength.

$4^{\text{th}}$ Layer. Defuzzification Layer. The product of normalized firing strength of the $3^{\text{rd}}$ layer and $p_i$, $q_i$, $r_i$ will be determined in this node.

$5^{\text{th}}$ Layer, Summation Layer. In the layer, permanent node with label $\Sigma$ sums all of the defuzzification outputs as an output signal [20].

**ANFIS training.** ANFIS training data are taken from Proportional Integral Differential (PID) control performance (as was performed by a previous research [12]).

Input model of the PID is a wide range frequency and peak of Aframax ship roll anggle. Instead of that, the input also represents sudden and uncertain wave. The PID run four times with different gains. As a result, there are three combined data. Those three data are $e_y$, $\Delta e_y$ and the compensator output. The $\Delta e_y$ is a calculation such as Equation (23).

Those $3 \times 1001$ data are trained using hybrid type in 17 epochs to get the best control performance. As the best result, the Fuzzy Inference System (FIS) is formed in 5 Gaussian type 2 membership functions. The FIS has 25 rules and 3.23 Mean Root Square Error (MRSE). The best ANFIS performance response is shown on Figure 5. The $\alpha_x$ ANFIS is an identical control with the $\alpha_y$ ANFIS.

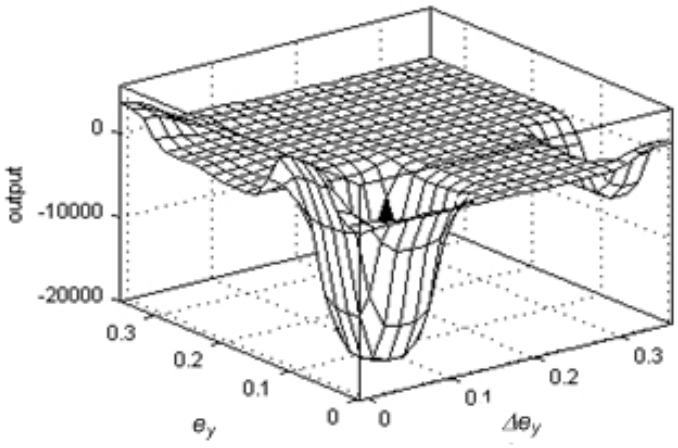


FIGURE 5. Wide range ANFIS surface

5. **Simulation and Result.** There are 3 simulations that are conducted to demonstrate the powerful and effectiveness of the proposed control. First simulation is to verify the focus achievement when the ship is under rough wave condition. Second simulation represents the immunity of the control toward engine vibration. And, the third simulation is to demonstrate the control stability in compensating panel position when the sun and the panel are in opposite direction or extreme position. In the simulations, the resting position of the tracker is on 0°.

5.1. **Rough wave response.** Figure 6 shows three mayor wave inputs in 200 seconds traveling simulation. Rough wave condition is a case, when a changing rate of wave degree toward time is extremely high above $1^{\circ}_{pp}$. Figure 6a) displays a rough roll model ($\phi$) of an Aframax tanker on the X axis. Figure 6b) demonstrates a violent pitch wave ($\theta$) of the tanker on the Y axis. Meanwhile, Figure 6c) illustrates an unexpected yaw movement ($\psi$) on the ship's z axis, which is caused by wave force or vessel's abrupt maneuver.

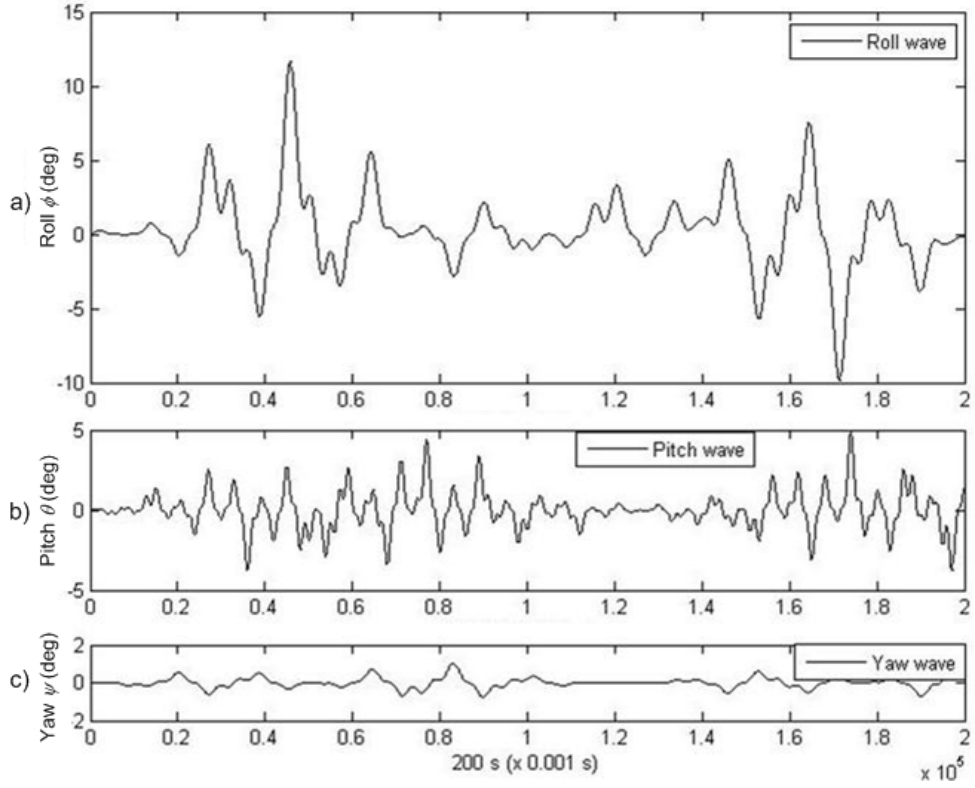


FIGURE 6. Roll ($\phi$), pitch ($\theta$) and yaw ($\psi$) of Aframax tanker

Due to the data validity test, the ANFIS performance is compared to PID action, which is as the source data training for the proposed control.

Figure 7a) demonstrates the ANFIS' $\alpha_y$ angle response on X axis, for 200 seconds. The method result performs excellence capability in compensating desired input within 0.006 degree error. In the same duration, the proposed method also shows perfect focus response in compensating roll input toward sun position, $\beta_y = 10$ deg, as shown on Figure 7b).

Similarly, the Y axis also shows accurate response in the same error value as X axis has, as displayed on Figure 8a). And also, its focus achievement responds well in adapting pitch wave toward sun angle, $\beta_x = -5^{\circ}$, that is shown on Figure 8b).

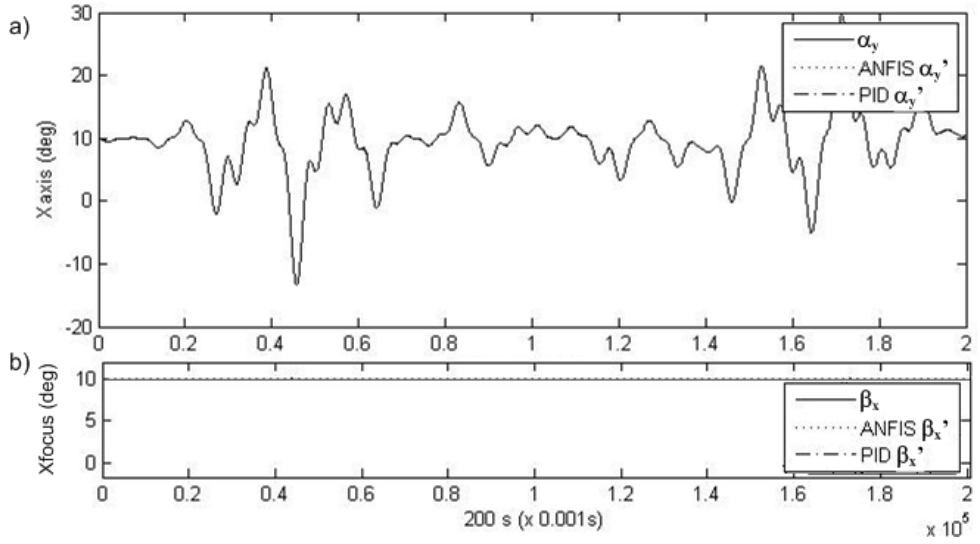


FIGURE 7. Actuator $\alpha_y$ and focus $\beta_y$ response

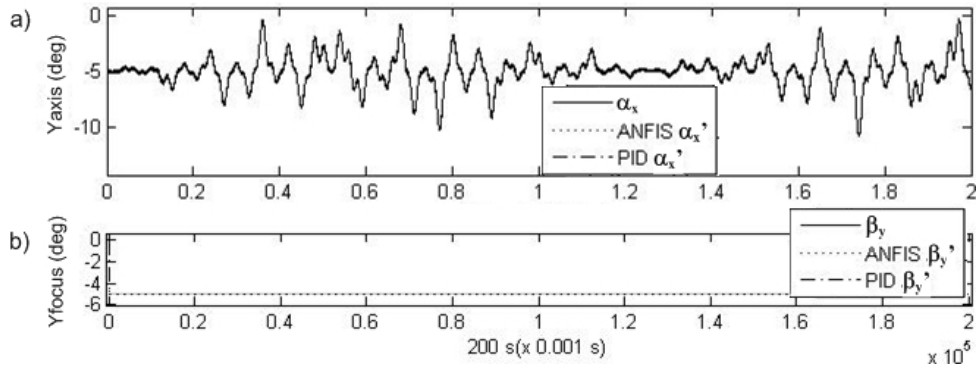


FIGURE 8. Actuator $\alpha_x$ and focus $\beta_x$ response

5.2. **Vibration immunity response.** Figures 9a) and 9b) show X and Y actuator response toward engine vibration $\varpi_y$ and $\varpi_x$. In holding the sun focus for HCPV panel, $\beta_y$ and $\beta_x$, ANFIS method performs excellence response as shown on Figures 9c) and 9d). Meanwhile, the conventional one shows unstable focus accuracy, especially there is high noise as displayed on Figure 9d). From the data analysis of the figures, it can be concluded that the sun focus accuracy performance, $\beta_y^{'}$ and $\beta_x^{'}$ reach 0.005 deg errors or 0.0028 percent error of 180 maximum degrees operation angle.

In the simulation result, Figure 9c) shows output response, $\beta_y^{'}$, toward its preferred input, $\beta_y$, when it is simulated with 0.1 $\deg_{pp}$ 10 Hz y direction engine vibration. Those graphs display the ANFIS' stability in locking the focus, even though there is a vibration. While the focus of the conventional one is exaggerated severely by the vibration as shown on Figure 9d).

Meanwhile, the same Figure 9d) also shows output response, $\beta_x^{'}$, toward its preferred input, $\beta_x$, when it is simulated on –5 $\deg_{pp}$ 9 spc pitch wave. Figures 9c) and 9d) prove that ANFIS has a very low distortion that is caused by engine vibration, especially in higher frequency, 20 Hz on $\beta_x$. The response is in the tolerated error, but the conventional one is out of the range. It means that ANFIS focus is not affected by engine vibration, but the PID is affected as high as the magnitude of the vibration itself.

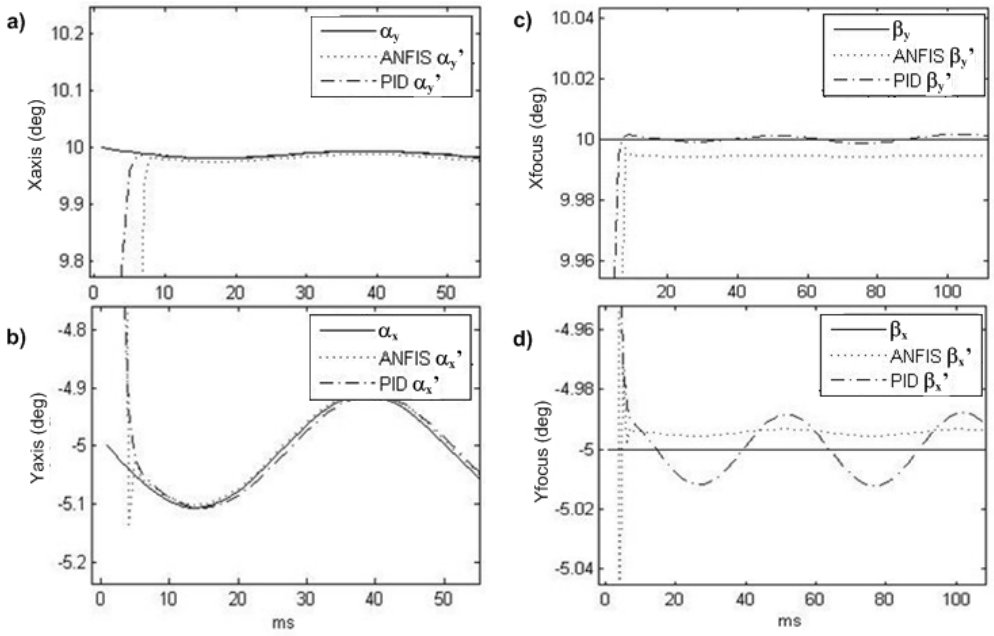


FIGURE 9. Axes and focus vibration response

TABLE 2. Variety period input response

| Period* | | Focus Error $\beta_x$ & $\beta_y$ ($\deg_{pp}$) | | $\alpha_x$ & $\alpha_y$ axis delay (s) | |
|---|---|---|---|---|---|
| cps | Hz | ANFIS | PID | ANFIS | PID |
| 20 | 0.05 | 0.005 | 0.0005 | 0.0001 | 0.0009 |
| 10 | 0.1 | 0.005 | 0.0005 | 0.0001 | 0.0009 |
| 1 | 1 | 0.006 | 0.004 | 0.0001 | 0.0009 |
| 0.1 | 10 | 0.006 | 0.06 | 0.0001 | 0.0009 |
| 0.05 | 20 | 0.007 | 0.06 | 0.0001 | 0.0009 |

* 0.5 $\deg_{pp}$ vibration.

In addition, further simulation, in Table 2, at ANFIS Focus error proves the stability of the proposed method for sun focus accuracy toward changing of wide range second per cycle input. It shows better focus error, only 0.002 degree rather than the conventional one, up to 0.065 deg. Furthermore, in the same table, the proposed method delay response indicates shorter delay response for only 0.0001 second constantly, while the other one is 0.0009 seconds.

5.3. **Extreme position response.** Extreme position occurs in a starting operation and cloudy condition. The extreme position means angle between sun position and solar tracker resting or previous position. Figure 10a) shows about ANFIS fast response on a high step degree input. Figure 10b) shows the ANFIS smooth and fast response performance in handling Y axes. The smaller step degree input, the faster the ANFIS response. While, Figure 10c) displays X axis' reached focus from 0° to 10° within 0.01 second, $\beta_y$. And also for Y axis, $\beta_x$, from 0° to −5° within 0.007 second, shown in Figure 10d).

The result of the further simulation on step input is presented in Table 3. The simulation is run with some extreme step inputs, in range of 1° to 180°. In the table, the ANFIS settling time shows an increment in increasing degree step of the axes. Instead of the settling time, the proposed method has an overshoot 0.06 deg or 0.03 percent of working

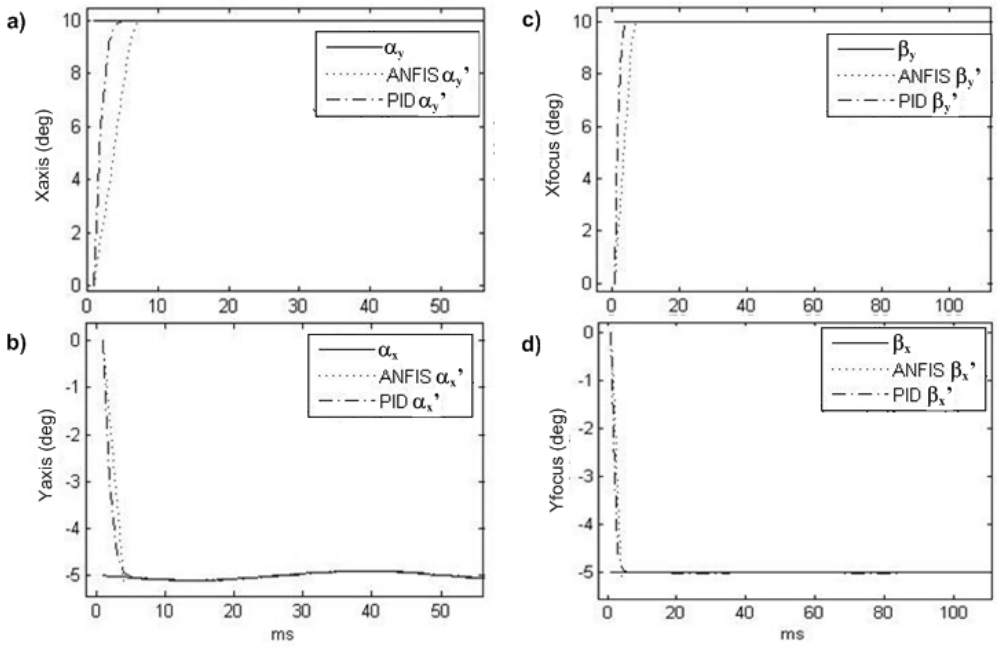


FIGURE 10. Axes and focus step response

TABLE 3. Step input response

| $\alpha_x$ &$\alpha_y$ | Overshot (deg) | | Settlingtime (s) | | Error (deg) | |
|---|---|---|---|---|---|---|
| (deg) | ANFIS | PID | ANFIS | PID | ANFIS | PID |
| 180 | 0.06 | 18 | 0.163 | 0.013 | 0.006 | 0.0003 |
| 90 | 0.06 | 0 | 0.080 | 0.006 | 0.006 | 0.0003 |
| 60 | 0.06 | 0 | 0.054 | 0.006 | 0.006 | 0.0003 |
| 30 | 0.06 | 0 | 0.028 | 0.006 | 0.006 | 0.0003 |
| 10 | 0.06 | 0 | 0.010 | 0.006 | 0.006 | 0.0003 |
| 1 | 0.06 | 0 | 0.003 | 0.004 | 0.006 | 0.0005 |

angle range. The overshot toward input degree step is stable. Finally, error happens in different degree of step input displays a stable peak 0.006 deg, or 0.003 percent of working range.

6. **Conclusion and Remark.** From the simulation and result, it has been proved that adaptive wide range ANFIS can handle non linear, time variant and uncertainty parameter of the ship's rotational movements in order to point the sun. The proposed method performs wider range wave period response, than the PID does. In addition, the proposed method also has vibration immunity on the focus performance with 0.0028 percent error, but the PID does not. In facing abrupt maneuver or starting condition, the proposed method presents high stability. The on-ship Cartesian tracker system has two axes, but it is capable to compensate ship's roll, pitch and yaw.

**Acknowledgment.** This research has been partially carried out under the support of Higher Education, Ministry of Education and Culture of Indonesia on Sandwich joint research program with Kumamoto University, Japan.

## REFERENCES


[1] B. Setiawan, M. H. Purnomo and M. Ashari, Artificial intelligent based modeling of mobile solar tracker for a large ship, *ICAST Proc. of International Student Conference on Advanced Science and Technology*, Ewha Womans University, Seoul, South Korea, pp.271-272, 2009.

[2] E. A. Katz, J. M. Gordon, W. Tassew and D. Feuermann, Photovoltaic characterization of concentrator solar cells by localized irradiation, *Journal of Applied Physic*, vol.100, pp.044514-1-044514-8, 2006.

[3] C. Algora, M. Baudrit, I. Rey-Stolle, D. Martn, R. Pea, B. Galiana and J. R. Gonzlez, Pending issues in the modeling of concentrator solar cells, *Journal for Process and Device Engineers*, vol.15, no.2, pp.1-11, 2005.

[4] W. A. Lynch and Z. M. Salaameh, Simple electro-optically controlled dual-axes sun tracker, *Pergamon Press, Solar Energy*, vol.45, no.2, pp.65-69, 1990.

[5] C.-Y. Lee, P.-C. Chou, C.-M. Chiang and C.-F. Lin, Sun tracking systems: A review, *Sensors*, vol.9, pp.3875-3890, 2009.

[6] H. Mousazadeh, A. Keyhani, A. Javadi, H. Mobli, K. Abrinia and A. Sharifi, A review of principle and sun-tracking methods for maximizing, *Elsevier Renewable and Sustainable Energy Reviews*, vol.13, pp.1800-1818, 2009.

[7] R. Y. Nuwayhid, F. Mrad and R. Abu-Said, The realization of a simple solar tracking concentrator for university research applications, *Elsevier, Pergamon, Renewable Energy*, vol.24, pp.207-222, 2001.

[8] P. Roth, A. Georgiev and H. Boudinov, Design and construction of a system for sun-tracking, *Elsevier, Renewable Energy*, vol.29, pp.393-402, 2004.

[9] F. R. Rubio, M. G. Ortega, F. Gordillo and M. Lopez-Martnez, Application of new control strategy for sun tracking, *Elsevier, Energy Conversion and Management*, vol.48, pp.2174-2184, 2007.

[10] A. Louchene, A. Benmakhlouf and A. Chaghi, Solar tracking system with fuzzy reasoning applied to crisp sets, *Revue des Energies Renouvelables*, vol.10, no.2, pp.231-240, 2007.

[11] A. Vasile, A. Drumea, C. Neacsu, M. Angel and D. A. Stoichescu, Automatic system and energetic efficiency optimization algorithm for solar panels on mobile systems, *IEEE Conferences on Electronics Technology, the 32nd International Spring Seminar*, pp.1-5, 2009.

[12] B. Setiawan, M. H. Purnomo and M. Ashari, PID based modeling performance for two axes mobile solar tracker on a large ship, *ICAST Proc. of International Student Conference on Advanced Science and Technology*, Edge University, Izmir, Turki, pp.339-340, 2010.

[13] M. Kratmuller, Adaptive fuzzy control design, *Acta Polytechnica Hungarica*, vol.6, no.4, pp.29-49, 2009.

[14] Y. Zhang, T. Chai, H. Niu and J. Zou, Nonlinear adaptive generalized predictive control method based on ANFIS and switching control, *Joint the 48th Conference on Decision and Control and the 28th Chinese Conference*, Shanghai, P. R. China, pp.4187-4192, 2009.

[15] S. Surendrana, S. K. Leeb, J. V. R. Reddyc and G. Leed, Non-linear roll dynamics of a Ro-Ro ship in waves, *Ocean Engineering*, vol.32, pp.1818-1828, 2005.

[16] M. S. Triantafyllou, M. Bodson and M. Athans, Real time estimation of ship motions using Kalman filtering techniques, *IEEE Journal of Ocean Engineering*, vol.8, no.1, pp.9-20, 1983.

[17] I. Senjanovic, J. Parunov and G. C. Chow, Safety analysis of ship rolling in rough sea, sohrons & fractals, *Elsevier Science Ltd PII*, vol.8, no.4, pp.659-680, 1997.

[18] R. A. Ibrahim and I. M. Grace, Review article modeling of ship roll dynamics and its coupling with heave and pitch, *Mathematical Problems in Engineering*, 2010.

[19] Oberstar, *DC Motor with Inertia Disk Model Development, Proportional Controller, and State Feedback Controller with Full State Estimator*, 2010.

[20] J.-S. R. Jang, *Neuro Fuzzy and Soft Computing, a Computational Approach to Learning and Machine Intelligent*, Prentice Hall, Upper Sadle River NJ 07458, 1997.